

A Two Level Finite Difference Scheme for One Dimensional Pennes' Bioheat Equation *

Jennifer J. Zhao †

Department of Mathematics and Statistics,
University of Michigan-Dearborn, Dearborn, MI 48374, USA

Jun Zhang ‡ Ning Kang §

Laboratory for High Performance Scientific Computing and Computer Simulation,
Department of Computer Science,
University of Kentucky, Lexington, KY 40506-0046, USA

Fuqian Yang ¶

Department of Chemical and Materials Engineering,
University of Kentucky, Lexington, KY 40506-0046, USA

September 20, 2002

Abstract

We develop a new two level finite difference scheme for the 1D Pennes' bioheat equation. We further prove that the scheme is stable and convergent unconditionally. Numerical experiments for a skin heating model are conducted.

Key words: bioheat transfer, Pennes' equation, finite difference.

2000 Mathematics Subject Classification: 90C10, 80A20, 65M06.

*Technical Report No. 354-02, Department of Computer Science, University of Kentucky, Lexington, KY, 2002.

†The research of this author was supported in part by the U.S. National Science Foundation under grant CCR-0117602. E-mail: xich@umich.edu, URL: <http://www.umd.umich.edu/~xich>.

‡The research of this author was supported in part by the U.S. National Science Foundation under grants CCR-9902022, CCR-9988165, CCR-0092532, and ACI-0202934, by the U.S. Department of Energy Office of Science under grant DE-FG02-02ER45961, by the Japanese Research Organization for Information Science & Technology, and by the University of Kentucky Research Committee. E-mail: jzhang@cs.uky.edu, URL: <http://www.cs.uky.edu/~jzhang>.

§The research of this author was supported in part by the U.S. Department of Energy Office of Science under grant DE-FG02-02ER45961. E-mail: nkang2@csr.uky.edu.

¶E-mail: fyang0@engr.uky.edu.

1 Introduction

Modern clinical treatments and medicines such as cryosurgery, cryopreservation, cancer hyperthermia, and thermal disease diagnostics, etc., require the understanding of thermal life phenomena and temperature behavior in living tissues [2, 4, 9]. Furthermore, skin burns caused by exposing human body to heat in a flash fire or being in contact with hot substances are some of the most commonly encountered hazards in daily life and in industry [7]. Therefore, studying bioheat transfer in human body has been a hot topic and is useful for effectively designing clinical thermal treatment equipments, for accurately evaluating skin burn, and for establishing thermal protections for various purposes.

Among the various models proposed to study the heat transfer in living tissues, the Pennes' equation is the most widely used one. It is based on the classical Fourier law [10], and has been greatly simplified after introducing the intuitive concept of blood perfusion, the blood flow rate per unit tissue volume, to study the bioheat transfer and assessment of skin burns.

The original one dimensional (1D) Pennes' equation [10] is given by:

$$\rho c \theta_t^* + w_b c_b \theta^* - (k(x) \theta_x^*)_x = Q_r, \quad 0 < x < L,$$

where ρ, c and k are the density, specific heat, and thermal conductivity of tissue, respectively. w_b and c_b are blood perfusion rate and specific heat of blood. Q_r is the volumetric heat due to spatial heating. $\theta^* = T - T_s$ is the elevated temperature, where T represents the temperature and T_s represents the skin's steady state temperature. L is the distance between skin surface and the body core. We assume that the thermal conductivity k depends on the space variable x only. We simplify the above equation by dividing both sides with ρc to get:

$$\theta_t^* + \frac{w_b c_b}{\rho c} \theta^* - \frac{1}{\rho c} (k(x) \theta_x^*)_x = \frac{Q_r}{\rho c},$$

which can be further simplified into:

$$\theta_t^* + \frac{w_b c_b}{\rho c} \left(\theta^* - \frac{Q_r}{w_b c_b} \right) - \frac{1}{\rho c} (k(x) \theta_x^*)_x = 0.$$

Assume that the volumetric heat Q_r to be constant and denote $\theta = \theta^* - \frac{Q_r}{w_b c_b}$, $a = \frac{w_b c_b}{\rho c} (> 0)$ and $b = \frac{1}{\rho c} (> 0)$, we can obtain the simplified form of the 1D Pennes' equation with initial and boundary conditions given below.

$$\theta_t + a\theta - b(k(x) \theta_x)_x = 0, \quad \theta(x, 0) = 0, \quad \theta(0, t) = \theta_0, \quad \theta_x|_{x=L} = 0. \quad (1)$$

Analytical solution of the 1D Pennes' equation is available in [8]. The trigonometric series based analytical solution is difficult and expensive to evaluate accurately. Liu et. al. [8] used a finite difference method to solve the Pennes' bioheat equation in a triple-layered skin structure composed of epidermis, dermis, and subcutaneous.

The three-layered skin model assumes three different values for the thermal conductivity parameter k , which is constant in a given layer. In our study, we assume that k is a continuous function of the skin tissue depth x , which is a more realistic model of human skin tissue [1], although an accurate representation of $k(x)$ is still needed.

Recently, Dai and Zhang [3] developed a three level unconditionally stable finite difference scheme and used a domain decomposition strategy for solving the 1D Pennes' equation for the same three-layered skin structure. In this paper, we construct a two level finite difference scheme for (1) which has the same order of accuracy as in [3]. Our scheme requires only one initial condition to start with, and is also unconditionally stable and convergent.

This paper is organized as follows. We construct a finite difference scheme for the Pennes' equation in Section 2. The solvability and stability of the scheme are proved in Section 3, and the convergence is proved in Section 4. Numerical experiments is reported in Section 5. Section 6 contains a brief summary.

2 Numerical Scheme

We use Δx to represent the space mesh and use N to represent an appropriate integer, such that $N \Delta x = L$. We construct a finite difference scheme for (1) by using the second order central difference scheme in space and the Crank-Nicholson type of scheme in time. For each interior grid point x_j , $0 < j < N$, the discretization scheme is:

$$\begin{aligned} \frac{\theta_j^{n+1} - \theta_j^n}{\Delta t} + \frac{a}{2} (\theta_j^{n+1} + \theta_j^n) \\ - \frac{b}{2} \left[\delta_x \left(k(x_{j+\frac{1}{2}}) \delta_x \theta_j^{n+1} \right) + \delta_x \left(k(x_{j+\frac{1}{2}}) \delta_x \theta_j^n \right) \right] = 0, \quad 0 < j < N, \end{aligned}$$

where δ_x is the central difference operator. For the two boundary points x_0 and x_N , the corresponding discretization schemes are:

$$\theta_0^{n+1} = \theta_0, \quad \frac{\theta_N^{n+1} - \theta_{N-1}^n}{\Delta x} = 0.$$

The difference scheme can be rewritten as:

$$\begin{aligned} \left(1 + \frac{a\Delta t}{2} \right) \theta_j^{n+1} - \frac{b\Delta t}{2\Delta x^2} \left[k(x_{j+1}) \theta_{j+1}^{n+1} - (k(x_j) + k(x_{j+1})) \theta_j^{n+1} + k(x_j) \theta_{j-1}^{n+1} \right] \\ = \left(1 - \frac{a\Delta t}{2} \right) \theta_j^n + \frac{b\Delta t}{2\Delta x^2} \left[k(x_{j+1}) \theta_{j+1}^n - (k(x_j) + k(x_{j+1})) \theta_j^n + k(x_j) \theta_{j-1}^n \right], \\ \theta_0^{n+1} = \theta_0, \quad \theta_N^{n+1} = \theta_{N-1}^n. \end{aligned} \quad (2)$$

The above schemes can be further simplified to the following form.

$$\begin{aligned} \theta_0^{n+1} = \theta_0, \\ \left(1 + \frac{a\Delta t}{2} + \frac{b}{2} \frac{\Delta t}{\Delta x^2} (k(x_j) + k(x_{j+1})) \right) \theta_j^{n+1} - \frac{b}{2} \frac{\Delta t}{\Delta x^2} k(x_j) \theta_{j-1}^{n+1} \\ - \frac{b}{2} \frac{\Delta t}{\Delta x^2} k(x_j) \theta_{j-1}^n \end{aligned}$$

$$\begin{aligned}
&= \left(1 - \frac{a\Delta t}{2} - \frac{b}{2} \frac{\Delta t}{\Delta x^2} (k(x_j) + k(x_{j+1}))\right) \theta_j^n + \frac{b}{2} \frac{\Delta t}{\Delta x^2} \theta_{j+1}^n \\
&\quad + \frac{b}{2} \frac{\Delta t}{\Delta x^2} k(x_j) \theta_{j-1}^n, \\
\theta_N^{n+1} &= \theta_{N-1}^n. \tag{3}
\end{aligned}$$

Our construction implies that the difference schemes have a truncation error in the order $O(\Delta x^2 + \Delta t^2)$ for each interior grid point (t^n, x_j) , $n \geq 1, 0 < j < N$.

3 Solvability and Stability

We prove the solvability and stability of (3) by introducing a vector which represents the numerical solutions at the time level t^n :

$$\vec{\theta}^n = \left(\theta_0^n, \dots, \theta_j^n, \dots, \theta_N^n\right)^T.$$

Here $\vec{\theta}^n$ is of size $N + 1$. Then the difference schemes (3) can be expressed in the following matrix form.

$$Q_L \vec{\theta}^n = Q_R \vec{\theta}^{n-1}, \quad n = 1, 2, \dots. \tag{4}$$

Here, Q_L and Q_R are both $(N + 1) \times (N + 1)$ square tridiagonal matrices which are given below.

$$Q_L = \begin{pmatrix} 1 & 0 & \cdots & \cdots & \cdots & 0 \\ \vdots & \vdots & \ddots & \ddots & \vdots & \vdots \\ 0 & \cdots & -\frac{b}{2} \frac{\Delta t}{\Delta x^2} k(x_j) & 1 + \frac{a\Delta t}{2} + \frac{b}{2} \frac{\Delta t}{\Delta x^2} (k(x_j) + k(x_{j+1})) & -\frac{b}{2} \frac{\Delta t}{\Delta x^2} k(x_{j+1}) & \cdots \\ \vdots & \vdots & \ddots & \ddots & \vdots & \vdots \\ 0 & \cdots & \cdots & \cdots & 0 & 1 \end{pmatrix}.$$

Here, each symbol \cdot represents 0, the first and the last diagonal element are both 1, and each diagonal element in between for the j th row is $1 + \frac{a\Delta t}{2} + \frac{b}{2} \frac{\Delta t}{\Delta x^2} (k(x_j) + k(x_{j+1}))$.

Similarly, Q_R is give by:

$$Q_R = \begin{pmatrix} 0 & \cdots & \cdots & \cdots & 0 \\ \vdots & \vdots & \ddots & \ddots & \vdots \\ \cdots & \frac{b}{2} \frac{\Delta t}{\Delta x^2} k(x_j) & 1 - \frac{a\Delta t}{2} - \frac{b}{2} \frac{\Delta t}{\Delta x^2} (k(x_{j+1}) + k(x_j)) & \frac{b}{2} \frac{\Delta t}{\Delta x^2} k(x_{j+1}) & \cdots \\ \vdots & \vdots & \ddots & \ddots & \vdots \\ 0 & \cdots & \cdots & \cdots & 1 \end{pmatrix}.$$

Here, each symbol \cdot represents 0, the first diagonal element is 0, the last diagonal element is 1. In between, the j th diagonal element is

$$1 - \frac{a\Delta t}{2} - \frac{b}{2} \frac{\Delta t}{\Delta x^2} (k(x_j) + k(x_{j+1}))$$

The solvability result is given in the next theorem.

Theorem 3.1 (4) is solvable for each time step n unconditionally.

Proof: To show the solvability of (4), we only need to prove that Q_L is invertible, we prove this by using the Gershgorin theorem ([5]).

It is clear that the first and last row of Q_L is diagonally dominant. For each other row, the diagonal element is

$$1 + \frac{a\Delta t}{2} + \frac{b}{2} \frac{\Delta t}{\Delta x^2} (k(x_j) + k(x_{j+1})), \quad 1 \leq j \leq N,$$

the sum of the absolute values of the off-diagonal elements on the same row are

$$\frac{b}{2} \frac{\Delta t}{\Delta x^2} (k(x_j) + k(x_{j+1})), \quad 1 \leq j \leq N.$$

Clearly, each row j , $1 \leq j \leq N$, is also diagonally dominant. So by the Gershgorin theorem, Q_L is invertible, this proves the solvability of the difference schemes. ■

We can further establish the following results which are proved in the **Appendix**.

Lemma 3.1 If $\lambda_{Q_L}^j$ and $\lambda_{Q_R}^j$, $j = 0, 1, \dots, N$, represent the eigenvalues of Q_L and Q_R respectively, and $\|\cdot\|_2$ represents the second matrix norm, then we have the following results.

$$|\lambda_{Q_L}^j| \geq 1 + \frac{a\Delta t}{2}, \quad 1 \leq j \leq N, \quad (5)$$

$$\|Q_L^{-1}\|_2 \leq \frac{1}{1 + \frac{a\Delta t}{2}} \leq 1 - a^* \Delta t < 1. \quad (6)$$

$$\|Q_R\|_2 \leq \max_{0 \leq j \leq N+1} \{\|\lambda_{Q_R}^j\|\} \leq 1. \quad (7)$$

a^* is some positive constant.

The stability result is stated in the next theorem.

Theorem 3.2 The schemes (3) are stable with respect to the initial data. In other words, $\vec{\theta}^n$ satisfies:

$$\|\vec{\theta}^n\|_2 \leq \|\vec{\theta}^0\|_2, \quad n \geq 1. \quad (8)$$

Proof: By the matrix form of the schemes (4), we have

$$\vec{\theta}^n = Q_L^{-1} Q_R \vec{\theta}^{n-1},$$

if we repeatedly use the above relation, we then get:

$$\vec{\theta}^n = (Q_L^{-1} Q_R) \vec{\theta}^{n-1} = \dots = (Q_L^{-1} Q_R)^n \vec{\theta}^0.$$

By using (5) to (7), we then get:

$$\|\vec{\theta}^n\|_2 \leq \|Q_L^{-1} Q_R\|_2^n \|\vec{\theta}^0\|_2 \leq \|Q_L^{-1}\|_2^n \|Q_R\|_2^n \|\vec{\theta}^0\|_2 \leq \|\vec{\theta}^0\|_2.$$

This shows that the difference schemes are unconditionally stable with respect to the initial data. ■

4 Convergence

To prove the convergence, we introduce another vector which represents the exact solution at the time t^n :

$$\vec{\theta}^{*n} = (\theta(x_0, t^n), \dots, \theta(x_j, t^n), \dots, \theta(x_N, t^n))^T,$$

this vector is also of size $N + 1$. Based on the construction of the schemes, we have

$$Q_L \vec{\theta}^{*n} = Q_R \vec{\theta}^{*n-1} + \vec{\tau}^n, \quad (9)$$

where $\vec{\tau}^n$ is the vector of the truncation errors at level t^n , $|\vec{\tau}^n| = O(\Delta t^2 + \Delta x^2)$. The convergence result is stated in the next theorem.

Theorem 4.1 *The schemes (3) are unconditionally convergent.*

Proof: If we subtract (4) from (9), we get

$$Q_L (\vec{\theta}^{*n} - \vec{\theta}^n) = Q_R (\vec{\theta}^{*n-1} - \vec{\theta}^{n-1}) + \vec{\tau}^n. \quad (10)$$

By introducing the error vector $\vec{E}^n = \vec{\theta}^{*n} - \vec{\theta}^n$, (10) can be manipulated to obtain:

$$\begin{aligned} \vec{E}^n &= Q_L^{-1} Q_R \vec{E}^{n-1} + Q_L^{-1} \vec{\tau}^n \\ &= (Q_L^{-1} Q_R) \left((Q_L^{-1} Q_R) \vec{E}^{n-2} + Q_L^{-1} \vec{\tau}^{n-1} \right) + Q_L^{-1} \vec{\tau}^n \\ &= \dots \\ &= (Q_L^{-1} Q_R)^n \vec{E}^0 + Q_L^{-1} \sum_{k=0}^{n-1} (Q_L^{-1} Q_R)^k \vec{\tau}^{n-k}. \end{aligned} \quad (11)$$

If we take $\vec{\theta}^0 = \vec{\theta}^{*0}$, then $\vec{E}^0 = \vec{0}$, and from (11), we obtain the following results.

$$\begin{aligned} \|\vec{E}^n\|_2 &\leq \|Q_L^{-1}\|_2 \left(\sum_{k=0}^{n-1} \|Q_L^{-1} Q_R\|_2^k \right) \max_{1 \leq m \leq n} \{\|\tau^m\|_2\} \\ &\leq \|Q_L^{-1}\|_2 \left(\sum_{k=0}^{n-1} \|Q_L^{-1}\|_2^k \|Q_R\|_2^k \right) \max_{1 \leq m \leq n} \{\|\tau^m\|_2\}. \end{aligned} \quad (12)$$

Since

$$\|Q_L^{-1}\|_2 < 1, \quad \|Q_R\|_2 \leq 1, \quad \|Q_L^{-1}\|_2 \leq \frac{1}{1 + \frac{a\Delta t}{2}} \leq 1 - a^* \Delta t,$$

for some positive constant a^* , we then get the following results from (12):

$$\|\vec{E}^n\|_2 \leq \left(\sum_{k=0}^{n-1} (1 - a^* \Delta t)^k \right) \max_{1 \leq m \leq n} \{\|\tau^m\|_2\} \leq e^{Cn\Delta t} \max_{1 \leq m \leq n} \{\|\tau^m\|_2\}. \quad (13)$$

by the Gronwall formula ([6]), C is come constant. Since

$$\lim_{\Delta t \rightarrow 0, \Delta x \rightarrow 0} \|\tau^m\|_2 = 0, \quad 1 \leq m \leq n, \quad (14)$$

this proves the convergence of the schemes. \blacksquare

5 Numerical Experiments

We solve the 1D Pennes' equation with the numerical discretization schemes developed as in Eq. (2). The model is a one dimensional skin structure with a thickness of $0.01208m$ [8]. The values of the physical properties in our test cases are chosen to be $\rho = 1000kg/m^3$, $c = c_b = 4200J/kg \cdot ^\circ C$, $w_b = 0.5kg/m^3$, $L = 0.01208m$, which are the same as those used in [8] except the thermal conductivity k , which is dependent on x . The step increase of the skin surface temperature is set to be $\theta_0 = 12^\circ C$. Since our purpose is to verify the stability of the developed finite difference schemes, we only consider the homogeneous tissue case [8] with the thermal conductivity of tissue being a function of the depth. The tests are performed on three meshes of 100, 1000, and 5000, respectively with the time increments being $\Delta t = 0.005$ and $\Delta t = 0.002$ for two different choices of $k(x)$.

We first choose $k(x) = 0.7(1 + 3x)$, which is a linear function of x , and the time step, Δt , to be $0.005s$. Fig. 1 shows the temperature elevations in the skin at $x = 0.00208m$. With three different mesh sizes, the results obtained by our two level finite difference scheme are almost on the same curve. The temperature profiles along the x direction at $150s$ are depicted in Fig. 2, which shows that the solutions are independent of the mesh sizes as well. In this test, the values of k are close to the step function (piecewise constant) used in [8]. The obtained temperature profile is similar to that reported in [8].

For the second test case, we set $k(x)$ to be a quadratic function of x , namely, $k(x) = 0.5 - (100x - 0.6)(100x - 0.5)$. The time increment is chosen to be $\Delta t = 0.002s$. The curves of temperature elevation in the skin at $x = 0.00208m$ are plotted in Fig. 3. Fig. 4 gives the temperature profiles along the x direction at $t = 150s$. We can see from both figures, which look similar to the corresponding figures in the previous test case, that the results do not depend on the mesh sizes. These results verify the stability of our difference schemes.

6 Summary

We have developed a new two level second order finite difference scheme for solving the one dimensional Pennes' bioheat equation. In our computation, we used a model that assumes continuity of thermal conductivity. This model avoids the discontinuity of thermal conductivity across the domain boundaries, which is the case in a three-layered skin model [3, 8]. Our computational results seem to agree with that computed by others with similar values of thermal conductivity.

We also proved the unconditional stability, solvability, and convergence of our scheme, which allows it to be used safely in this application.

We remark that our two level finite difference method should be equally applicable in a three-layered skin structure modeling by employing the idea of domain decomposition as in [3].

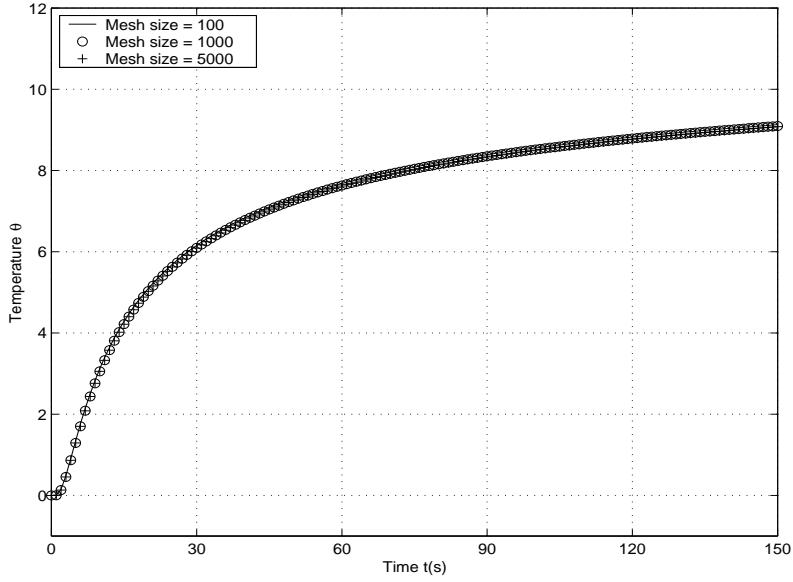


Figure 1: Temperature elevations in the skin at $x = 0.00208m$, with $k(x) = 0.7(1 + 3x)$ and $\Delta t = 0.005s$.

Appendix

We now prove the inequalities (5) to (7). The Gershgorin theorem states that each eigenvalue λ of a square matrix $A = (a_{ij})_{M \times M}$ is in at least one of the following disks,

$$|\lambda - a_{jj}| \leq \sum_{l=1, l \neq j}^M |a_{lj}|, \quad j = 1, 2, \dots, M.$$

This implies that each eigenvalue at least satisfies one of the following inequalities:

$$|\lambda| \leq |\lambda - a_{jj}| + \sum_{l=1, l \neq j}^M |a_{lj}| \leq \sum_{l=1}^M |a_{lj}|, \quad 1 \leq j \leq M, \quad (15)$$

and:

$$|\lambda| \geq |a_{jj}| - |\lambda - a_{jj}| \geq |a_{jj}| - \sum_{l=1, l \neq j}^M |a_{lj}|, \quad 1 \leq j \leq M. \quad (16)$$

If we apply (16) to Q_L , we get that each eigenvalue of Q_L satisfies at least one of the following inequalities:

$$|\lambda| \geq 1, \quad j = 0, \text{ and } N + 1, \quad (17)$$

$$|\lambda| \geq 1 + \frac{a \Delta t}{2}, \quad 1 \leq j \leq N. \quad (18)$$

Since

$$\|Q_L\|_2 = \max_{0 \leq j \leq N+1} \{|\lambda_{Q_L}^j|\},$$

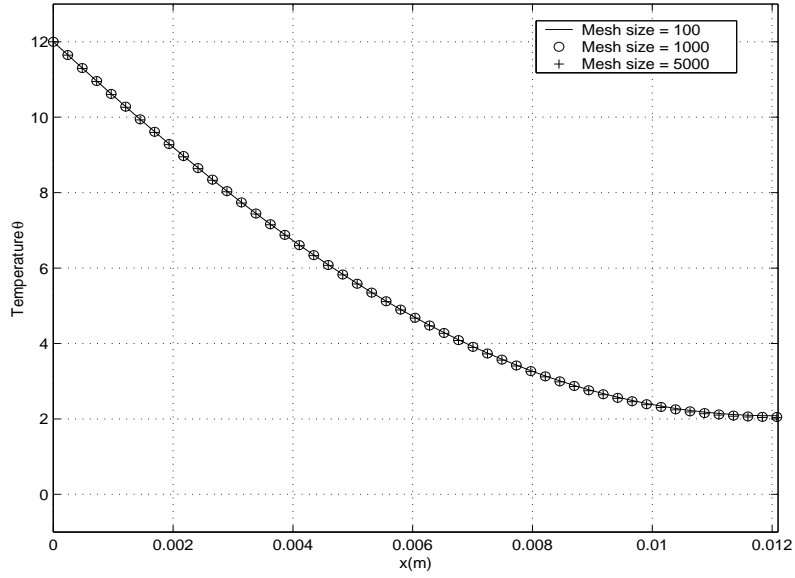


Figure 2: Temperature profiles along the x direction at $t = 150s$, with $k(x) = 0.7(1 + 3x)$ and $\Delta t = 0.005s$.

and without losing generality, we can assume that at least one of the eigenvalues of Q_L satisfies (18), then it follows that

$$\|Q_L\|_2 \geq 1 + \frac{a\Delta t}{2}.$$

This proves (5) and (6) follows from this result. The inequality (7) can be proved similarly by applying (15) to Q_R .

References

- [1] B. Büttner, Effects of extreme heat on man, *JAMA*, 144:732–738, 1950.
- [2] J. C. Chato, *Fundamentals of Bioheat Transfer*, Springer-Verlag, Berlin, 1989.
- [3] W. Z. Dai and J. Zhang, A three level finite difference scheme for solving the Pennes' bioheat transfer in a triple-layered skin structure, Technical Report No. 343-02, Department of Computer Science, University of Kentucky, Lexington, KY, 2002.
- [4] M. Gautherie, *Clinical Thermology: Thermotherapy*, Vol. 1–4, Springer-Verlag, Heidelberg, 1990.
- [5] M. T. Heath, *Scientific Computing, An Introductory Survey*, 2nd ed., McGraw-Hill, New York, NY, 2002.
- [6] P. Holmes, *Nonlinear Oscillations, Dynamical Systems and Bifurcations of Vector Fields*, Springer-Verlag, Boston, MA, 1983.

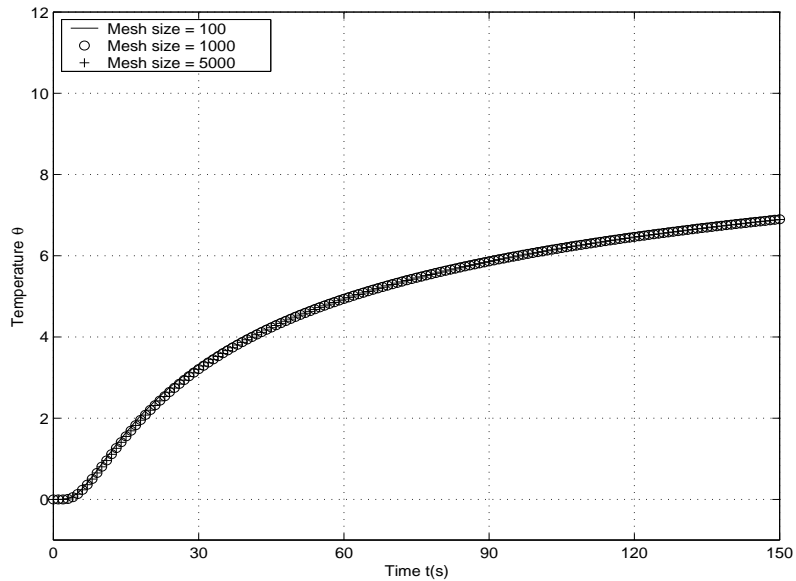


Figure 3: Temperature elevations in the skin at $x = 0.01208m$, with $k(x) = 0.5 - (100x - 0.6)(100x - 0.5)$ and $\Delta t = 0.002s$.

- [7] K. R. Killer and L. J. Hayes, Analysis of tissue injury by burning: comparison of *in situ* and skin flap models, *Int. J. Heat Mass Transfer*, 34:1393–1406, 1991.
- [8] J. Liu, X. Chen, and L. X. Xu, New thermal wave aspects on burn evaluation of skin subjected to instantaneous heating, *IEEE Trans. Biomed. Engrg.*, 46:420–428, 1999.
- [9] M. Miyakawa and J. C. Bolomey (Eds.), *Non-Invasive Thermometry of Human Body*, CRC Press, Boca Raton, 1996.
- [10] H. H. Pennes, Analysis of tissue and arterial temperature in the resting human forearm, *J. Appl. Physiol.*, 1:93–122, 1948.

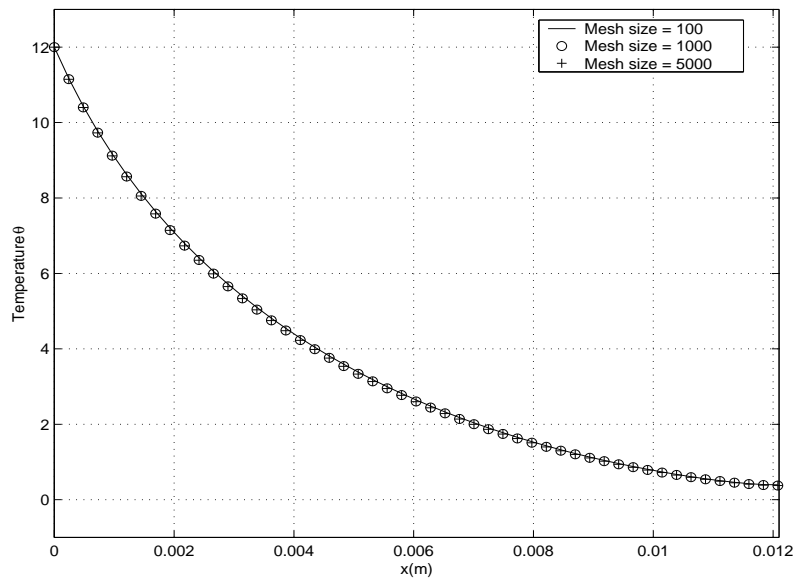


Figure 4: Temperature profiles along the x direction at $t = 150s$, with $k(x) = 0.5 - (100x - 0.6)(100x - 0.5)$ and $\Delta t = 0.002s$.